Article

Iridium(0) Nanocluster, Acid-Assisted Catalysis of Neat Acetone Hydrogenation at Room Temperature: Exceptional Activity, Catalyst Lifetime, and Selectivity at Complete Conversion

Saim zkar, and Richard G. Finke

J. Am. Chem. Soc., **2005**, 127 (13), 4800-4808• DOI: 10.1021/ja0437813 • Publication Date (Web): 08 March 2005

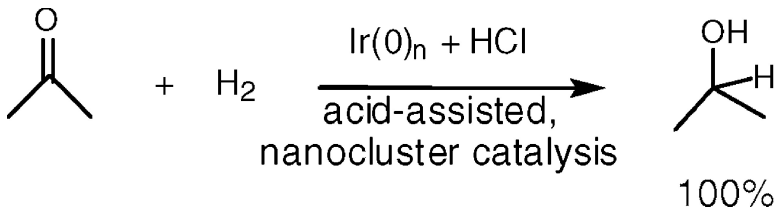

More About This Article

Additional resources and features associated with this article are available within the HTML version:

- Supporting Information
- Links to the 4 articles that cite this article, as of the time of this article download
- Access to high resolution figures
- Links to articles and content related to this article
- Copyright permission to reproduce figures and/or text from this article

View the Full Text HTML

J|A|C|S
ARTICLES
Published on Web 03/08/2005

Iridium(0) Nanocluster, Acid-Assisted Catalysis of Neat Acetone Hydrogenation at Room Temperature: Exceptional Activity, Catalyst Lifetime, and Selectivity at Complete Conversion

Saim Özkar† and Richard G. Finke*,‡

Contribution from the Departments of Chemistry, Middle East Technical University, 06531 Ankara, Turkey, and Colorado State University, Fort Collins, Colorado 80523

Received October 12, 2004; E-mail: rfinke@lamar.colostate.edu

Abstract: Acetone hydrogenation catalysis is important in applications such as heat pumps and fuel cells or in fulfilling the sizable demand for the product of selective acetone hydrogenation, 2-propanol. Reported herein is the discovery of a superior acetone hydrogenation catalyst— superior in terms of activity at low temperature, selectivity at complete conversion, and total catalyst lifetime. The new catalyst system consists of $Ir(0)_n$ nanoclusters plus HCl easily and reproducibly formed from commercially available $[(1,5\text{-COD})\text{-IrCl}]_2$ under H_2. The resultant, room temperature, high activity, and highly selective $(2/n)Ir(0)_n$ plus 2HCl catalyst system hydrogenates acetone at 22 °C and 40 psig of H_2 pressure to 95% 2-propanol and the rest diisopropyl ether at 100% conversion with 16400 total catalytic turnovers and with an initial turnover frequency of 1.9 s^{-1} at 22 °C. When molecular sieves are added, the catalyst system becomes even more selective and long-lived, providing the complete and selective conversion of acetone to 100% 2-propanol with 188000 total turnovers. Also reported are initial kinetic, D-labeling and other mechanistic studies, a summary section detailing the four main findings, the "green chemistry" aspects, and the current main drawback (a limited catalytic lifetime due to nanocluster precipitation) of the present invention. A review of the extensive literature of acetone hydrogenation is also tabulated as part of the Supporting Information.

Introduction

The catalytic hydrogenation of acetone is an important reaction, one used to produce two industrial chemicals, 2-propanol[1] and, at higher temperature (as a result of acetone condensation, dehydration, and subsequent hydrogenation), methyl isobutyl ketone ($(CH_3)_2CHCH_2C(O)CH_3$).[2] In addition, acetone hydrogenation to 2-propanol is of interest for use in chemical heat pumps[3] or fuel cells,[4] applications which require a higher selectivity to 2-propanol at high conversion than is presently available.[3] The demand for 2-propanol is also increasing due to its transfer hydrogenation reactions,[5] chemistry which exploits 2-propanol's relatively easy, selective reoxidation to acetone.[6]

A range of heterogeneous or homogeneous catalysts have been used to hydrogenate acetone, commonly at temperatures in the 100−300 °C range for heterogeneous catalysts; see Table S-1 of the Supporting Information, where the results and conditions for 14 of the best, prototype prior acetone hydrogenation catalyst systems are tabulated from among >340 citations resulting from a SciFinder literature search of "acetone hydrogenation": Raney Ni, $[Ir(CO)(PPh_3)_3]ClO_4$, $[Rh_2(CO)_2(dppm)_3]^+$, 8−15% Ni/SiO_2, 0−50% Ni/Al_2O_3, Pt/zeolite, Pt/SiO_2, 10−50% Ni or Co or Fe/Al_2O_3, Tc or Tc−M (M = Pt, Pd, Rh, Ru, Ni, Re, Co)/Al_2O_3 (or supported on SiO_2 or MgO), Ni/β-zeolite (or zeolite-Y), CoMgAl or NiMgAl layered double hydroxides, $CuCr_2O_4$, $Cu_6O_8Ln(NO_3)$, and Pt/actived carbon. The resultant products are typically 2-propanol and methyl isobutyl ketone plus other products (methyl isobutyl carbinol,

† Middle East Technical University.
‡ Colorado State University.

(1) Anderson, L. C.; MacNaughton, N. W. *J. Am. Chem. Soc.* **1942**, *64*, 1456.
(2) Methyl isobutyl ketone is used as a solvent for vinyl, epoxy, and acrylic resins as well as cellulose-based coatings. (a) Gandia, L. M.; Montes, M. *Appl. Catal., A: General* **1993**, *101*, L1. (b) Reith, W.; Dettmer, M.; Widdecke, H.; Fleischer, B. *Stud. Surf. Sci. Catal.* **1991**, *59*, 487.
(3) Note that the preferred operating temperature in the heat-pump application is around 200 °C: (a) Wojcik, A. M. W.; van der Koi, H. J.; Maschmeyer, T. *J. Phys. D: Appl. Phys.* **2001**, *34*, 660−666. (b) Gandia, L. M.; Montes, M. *Int. J. Energy Res.* **1992**, *16*, 851−864. (c) Meng, N.; Shinoda, S.; Saito, Y. *Int. J. Hydrogen Energy* **1997**, *22*, 361−367. (d) Chung, Y.; Kim, B. J.; Yeo, Y. K.; Song, H. K. *Energy* **1997**, *22*, 525−536.
(4) (a) Ando, Y.; Tanaka, T.; Doi, T.; Takashima, T. *Energy Convers. Manage.* **2001**, *42*, 1807−1816. (b) Pardillos-Guindet, J.; Metais, S.; Vidal, S.; Court, J.; Foulloux, P. *Appl. Catal., A* **1995**, *132*, 61−75. (c) Pardillos-Guindet, J.; Vidal, S.; Court, J.; Foulloux, P. *J. Catal.* **1995**, *155*, 12−20.
(5) Reviews: (a) Birch, A. J.; Williamson, D. H. *Org. React. (N. Y.)* **1976**, *24*, 1−186. (b) Matteoli, U.; Frediani, P.; Binachi, M.; Botteghi, C.; Gladiali, S. *J. Mol. Catal.* **1981**, *12*, 265−319. (c) Zassinovich, G.; Mestroni, G.; Gladiali, S. *Chem. Rev.* **1992**, *92*, 1051−1069. (d) de Graauw, C. F.; Peters, J. A.; van Bekkum, H.; Huskens, J. *Synthesis* **1994**, 1007−1017. (e) Gladiali, S.; Mestroni, G. *Transition Met. Org. Synth.* **1998**, *2*, 97−119. (f) Palmer, M. J.; Wills, M. *Tetrahedron: Asymmetry* **1999**, *10*, 2045−2061. (g) Wills, M.; Palmer, M.; Smith, A.; Kenny, J.; Walsgrove, T. *Molecules* **2000**, *5*, 4−18. (h) Wills, M.; Gamble, M.; Palmer, M.; Smith, A.; Studley, J.; Kenny, J. *J. Mol. Catal. A* **1999**, *146*, 139−148. (i) Fache, F.; Schulz, E.; Tommasino, M. L.; Lemaire, M. *Chem. Rev.* **2000**, *100*, 2159−2231. (j) Casey, C. P.; Johnson, J. B. *J. Org. Chem.* **2003**, *68*, 1998.
(6) (a) Wilds, A. L. *Org. React. (N. Y.)* **1944**, *2*, 178−223. (b) Djerassi, C. *Org. React. (N. Y.)* **1951**, *6*, 207−272. (c) Namy, J. L.; Souppe, J.; Collin, J.; Kagan, H. B. *J. Org. Chem.* **1984**, *49*, 2045−2049. (d) Hallman, P. S.; McGarvey, B. R.; Wilkinson, G. *J. Chem. Soc. A* **1968**, 3143−3150.

10.1021/ja0437813 CCC: $30.25

diacetone alcohol, mesityl oxide, diisobutyl ketone, propane, and 2-methylpentane) in ratios which depend on the reaction conditions.[7−15] The selectivity at lower temperatures typically favors 2-propanol, while higher temperatures favor methyl isobutyl ketone;[8c,9a] however, an interesting reversal of selectivity from 100% 2-propanol at 90% conversion for 10% Ni/Al_2O_3 to 4% 2-propanol and 96% methyl isobutyl ketone for 50% Ni/Al_2O_3 at 100 °C has been reported.[9c] The best selectivity at the highest conversion previously reported is 100% 2-propanol at 90% conversion at 100 °C for the above-noted 50%Ni/Al_2O_3 system;[9a,c] the second-best is 97% selectivity at 65% conversion at 100 °C for a bimetallic 0.2% Rh/0.2% Tc/γ-Al_2O_3 catalyst.[12] Activities (turnover frequency (TOF), s^{-1}) are reported for only 3 out of the 14 examples in Table S-1 of the Supporting Information, the highest previous reported activity being a TOF = 8.5 s^{-1} at 100 °C for Pt/activated carbon[11] and 11 s^{-1} at 200 °C for Ni/SiO_2.[8c] The general trend for acetone hydrogenation activity (for at least γ-Al_2O_3-supported metals) is reported to be Pt > Tc ≈ Rh > Pd > Ru > Ni ≈ Re > Co.[12] The very important catalysis parameter of catalytic lifetime (i.e., total turnover number, TTO) for acetone hydrogenation has not been specifically reported in the prior literature. In short, without prior precedent and thus of considerable interest are acetone hydrogenation catalysts which operate at room temperature, with an activity ≥8.5 s^{-1} at ≤100 °C, with selectivites to 2-propanol ≥95% for 100% conversions, and which exhibit extended catalytic lifetimes.

Herein we report our discovery that a chloride-stabilized[16] Ir(0) nanocluster[17−20] catalyst is the lowest temperature, most active, highest selective at high (100%) conversion, and longest lifetime catalyst yet reported for acetone hydrogenation to 2-propanol.[21,22] Our iridium(0) nanoclusters are easily and reproducibly formed in situ in neat acetone by the hydrogen reduction of the commercial (1,5-cyclooctadiene)chloroiridium-(I) dimer precatalyst, $[(1,5\text{-COD})IrCl]_2$, at 22 °C and 40 psig of H_2 pressure. Reduction of the $[(1,5\text{-COD})IrCl]_2$ by H_2 yields 1 equiv of H^+Cl^- for each Ir(I) reduced to iridium(0); the result is a highly efficient, acid-assisted, high-selectivity acetone hydrogenation catalyst. Nanocluster catalysis of acetone hydrogenation has not been previously reported prior to our disclosure in 1999 in a footnote that we had observed this reaction using Ir and Rh nanoclusters for the first time[21] and our brief citation, in 2001, that the present study was in progress (see footnote 52 on p 5806 in ref 22). Small molecules that can store H_2, such as an acetone/2-propanol couple, are also of general interest regarding a future H_2 economy, especially if such couples proceeed with 100% conversion and the absence of side products.[23]

(7) Raney nickel as catalyst: (a) Freund, T.; Hulburt, H. M. *J. Phys. Chem.* **1957**, *61*, 909. (b) Kishida, S.; Teranishi, S. *J. Catal.* **1968**, *12*, 90. (c) Lemcoff, N. O. *J. Catal.* **1977**, *46*, 356−364.

(8) Silica-supported Co, Ni, Cu, Rh, Pd, Pt, and Au catalysts: (a) Van Druten, G. M. R.; Ponec, V. *React. Kinet. Catal. Lett.* **1999**, *68*, 15−23. (b) Van Druten, G. M. R.; Aksu, L.; Ponec, V. *Appl. Catal., A* **1997**, *149*, 181−187. (c) Gandia, L. M.; Diaz, A.; Montes, M. *J. Catal.* **1995**, *157*, 461−471. (d) Nakamura, M.; Wise, H. In *Proceedings of the 6th International Congress on Catalysis*, London, 1976; Bond, G. C., Wells, P. B., Tompkins, F. C., Eds.; The Chemical Society: London, 1977; p 881. (e) Simoikova, J.; Hillaire, L.; Panek, J.; Kochleofl, K. *Z. Phys. Chem. FR* **1973**, *83*, 287−304. (f) Sen, B.; Vannice, M. A. *J. Catal.* **1988**, *113*, 52−71.

(9) Alumina-supported Ni, Co, and Fe catalysts: (a) Narayan, S.; Unnikrishnan, R. *J. Chem. Soc., Faraday Trans.* **1998**, *94*, 1123−1128. (b) Narayan, S.; Unnikrishnan, R. *Stud. Surf. Sci. Catal.* **1998**, *113*, 799−807. (c) Narayan, S.; Unnikrishnan, R. *Appl. Catal., A* **1996**, *145*, 231−236.

(10) Layered double hydroxide containing Co, Ni, Mg, and Al as catalysts: Unnikrishnan, R.; Narayan, S. *J. Mol. Catal.* **1999**, *144*, 173−179.

(11) Activated carbon-supported Pt catalysts: Fuente, A. M.; Pulgar, G.; Gonzalez, F.; Pesquera, C.; Blanco, C. *Appl. Catal., A* **2001**, *208*, 35−46.

(12) Tc or Tc−M (M = Pt, Pd, Rh, Ru, Ni, Re, Co) supported on Al_2O_3, SiO_2, or MgO as catalysts: (a) Rimar, N. N.; Pirogova, G. N. *Russ. Chem. Bull.* **1998**, *47*, 398−401. (b) Pirogova, G. N.; Popova, N. N.; Voronin, Y. V. *Radiochemistry* **2000**, *42*, 565−568.

(13) Zeolites containing transition-metal catalysts: (a) Melo, L.; Magnoux, P.; Giannetto, G.; Alvarez, F.; Gusinet, M. *J. Mol. Catal., A* **1997**, *124*, 155−161. (b) Knifton, J. F.; Dai, P. S. E. *Catal. Lett.* **1999**, *57*, 193−197.

(14) Copper compounds such as $CuCr_2O_4$ and $Cu_6O_8Ln(NO_3)$ as catalysts: (a) Yurieva, T. M. *Catal. Today* **1999**, *51*, 457−467. (b) Yurieva, T. M. *J. Mol. Catal., A* **1996**, *113*, 455−468. (c) Sakata, Y.; Nobukuni, S.; Kikumoto, E.; Tanak, K.; Imamura, H.; Tsuchiya, S. *J. Mol. Catal., A* **1999**, *141*, 269−276.

(15) Homogeneous catalysts, including Noyori's transfer-hydrogenation catalysts,[15e−i] are listed below. References 38 and 39 provided additional systems, many of which probe the underlying mechanisms of ketone hydrogenation. (a) Chin, C. S.; Park, S. C. *Bull. Korean Chem. Soc.* **1988**, *9*, 260−261. (b) Geraty, S. M.; Harkin, P.; Vos, J. G. *Inorg. Chim. Acta* **1987**, *131*, 217−220. (c) Harman, W. D.; Taube, H. *J. Am. Chem. Soc.* **1990**, *112*, 2261. (d) Shafiq, F.; Eisenberg, R. *J. Organomet. Chem.* **1994**, *472*, 337−345. (e) Haack, K. J.; Hashiguchi, S.; Fuji, A.; Ikeriya, T.; Noyori, R. *Angew. Chem., Int. Ed. Engl.* **1997**, *36*, 285−288. (f) Noyori, R., Hashiguchi, S. *Acc. Chem. Res.* **1997**, *30*, 97. (g) Matsumura, K.; Hashiguchi, S.; Noyori, R. *J. Am. Chem. Soc.* **1997**, *119*, 8738. (h) Yamakawa, M.; Ito, M.; Noyori, R. *J. Am. Chem. Soc.* **2000**, *122*, 1466. (i) Noyori, R., Yamakawa, M.; Hashiguchi, S. *J. Org Chem.* **2001**, *66*, 7931.

(16) Chloride anion is a common nanocluster stabilizer, albeit not one of the best:[22] Schmid, G.; Harms, M.; Malm, J. O.; Bovin, J. O.; van Ruitenbeck, J.; Zandbergen, H. W.; Fu, W. T. *J. Am. Chem. Soc.* **1993**, *115*, 2046.

(17) Representative reviews or papers on nanocluster catalysis: (a) Templeton, A. C.; Wuelfing, W. P.; Murray, R. W. *Acc. Chem. Res.* **2000**, *33*, 27. (b) Rao, C. N. R.; Kulkarni, G. U.; Thomas, P. J.; Edwards, P. P. *Chem. Soc. Rev.* **2000**, *29*, 27. (c) Schmid, G.; Baumle, M.; Geerkens, M.; Heim. I.; Osemann, C.; Sawitowski, T. *Chem. Soc. Rev.* **1999**, *28*, 179. (d) Stein, J.; Lewis, L. N.; Gao, Y.; Scott, R. A. *J. Am. Chem. Soc.* **1999**, *121*, 3693. (e) Reetz, M. T.; Breinbauer, R.; Wedemann, P.; Binger, P. *Tetrahedron* **1998**, *54*, 1233. (f) Schmidt, T. J.; Noeske, M.; Gasteiger, H. A.; Behm, R. J.; Britz, P.; Brijoux, W.; Bönnemann, H. *Langmuir* **1997**, *13*, 2591. (g) Schmid, G.; Maihack, V.; Lantermann, F.; Peschel, S. *J. Chem. Soc., Dalton Trans.* **1996**, 589. (h) Reetz, M. T.; Breinbauer, R.; Wanninger, K. *Tetrahedron Lett.* **1996**, *37*, 4499. (i) Reetz, M. T.; Quaiser, S. A.; Merk, C. *Chem. Ber.* **1996**, *129*, 741. (j) Bönnemann, H.; Braun, G. A. *Angew. Chem., Int. Ed. Engl.* **1996**, *35*, 1992. (k) Lewis, L. N. *Chem. Rev.* **1993**, *93*, 2693.

(18) For two introductory reviews, lead references to earlier reviews, and needed definitions (e.g., of modern transition-metal nanoclusters vs, for example, classical colloids), see: (a) Aiken, J. D., III; Finke, R. G. *J. Mol. Catal. A* **1999**, *145*, 1. (b) Aiken, J. D., III; Lin, Y.; Finke, R. G. *J. Mol. Catal. A* **1996**, *114*, 29−51. (c) Finke, R. G. In *Metal Nanoparticles: Synthesis, Characterization and Applications*; Feldheim, D. L., Foss, C. A., Jr., Eds.; Marcel Dekker: New York, 2002; Chapter 2, pp 17−54 (Transition-Metal Nanoclusters: Solution-Phase Synthesis, then Characterization and Mechanism of Formation, of Polyoxoanion- and Tetrabutylammonium-Stabilized Nanoclusters).

(19) Reviews (see also ref 18): (a) Bönnemann, H.; Richards, R. *Eur. J. Inorg. Chem.* **2001**, 2455. (b) Schmid, G.; Baumle, M.; Geerkens, M.; Heim, I.; Osemann, C.; Sawitowski, T. *Chem. Soc. Rev.* **1999**, *28*, 179. (c) Schmid, G.; Chi, L. F. *Adv. Mater.* **1998**, *10*, 515. (d) Fendler, J. H., Ed. *Nanoparticles and Nanostructured Films*; Wiley-VCH: Weinheim, Germany, 1998. (e) Fürstner, A., Ed. *Active Metals: Preparation, Characterization, and Applications*; VCH: Weinheim, Germany, 1996. (f) Bradley, J. S. In *Clusters and Colloids. From Theory to Applications*; Schmid, G., Ed.; VCH: New York, 1994; pp 459−544. (g) Schmid, G. *Chem. Rev.* **1992**, *92*, 1709. (h) A superb series of papers is available in *Faraday Discuss.* **1991**, *92*, 1−300. (i) Schmid, G. In *Aspects of Homogeneous Catalysis*; Ugo, R., Ed.; Kluwer: Dordrecht, The Netherlands, 1990; Chapter 1. (j) Andres, R. P.; Averback, R. S.; Brown, W. L.; Brus, L. E.; Goddard, W. A.; Kaldor, A.; Louie S. G.; Moscovits, M.; Peercy, P. S.; Riley, S. J.; Siegel, R. W.; Spaepen, F.; Wang, Y. *J. Mater. Res.* **1989**, *4*, 704. (k) Henglein, A. *Chem. Rev.* **1989**, *89*, 1861. (l) Thomas, J. M. *Pure Appl. Chem.* **1988**, *60*, 1517. (m) Jena, P.; Rao B. K.; Khanna, S. N. *Physics and Chemistry of Small Clusters*; Plenum: New York, 1987.

(20) See ref 18 for a review of nanocluster catalysis which includes necessary key terms and definitions of nanoclusters vs traditional (nano-) colloids, monodisperse (±0% size distribution) and near-monodisperse (≤±15% size distribution) nanoparticles, and "magic number" (i.e., full shell and thus enhanced stability) nanoclusters, Schwartz's updated definition of homogeneous vs heterogeneous catalysts, and definitions of inorganic ("charge") and organic ("steric") stabilization mechanisms for colloids and nanoparticles.

(21) Acetone as well as acetonitrile hydrogenation by both Ir and Rh nanoclusters was first noted in footnote 27 and Table B in Aiken, J. D., III; Finke, R. G. *Chem. Mater.* **1999**, *11*, 1035.

(22) (a) Özkar, S.; Finke, R. G. *J. Am. Chem Soc.* **2001**, *124*, 5796. (b) Özkar, S.; Finke, R. G. *Langmuir* **2002**, *18*, 7653−7662.

(23) *Basic Research Needs For the Hydrogen Economy*; Report of the Basic Energy Sciences Workshop on Hydrogen Production, Storage and Use, May 13−15, 2003; Office of Science, U.S. Department of Energy: Washington, DC, 2003; www.sc.doe.gov/bes/ hydrogen.pdf.

Results and Discussion

Acetone Hydrogenation Products, Selectivity, Conversion, and Yield. In what we will hereafter term a standard conditions[24] nanocluster formation and concomitant acetone hydrogenation experiment $[(1,5\text{-COD})IrCl]_2$ (3.6 μmol Ir) was placed in neat acetone (0.5 mL, 6.7 mmol) in a Fischer−Porter (F−P) pressure bottle along with a stir bar, all while working inside a $\leq$1 ppm O_2 inert-atmosphere N_2 drybox. The F−P bottle was then sealed, removed from the drybox, and attached to a computer-interfaced pressure transducer apparatus that has been described in detail previously.[22,25] The F−P bottle was thermostated at 22 ± 0.1 °C, and an Ir(0) nanocluster formation and acetone hydrogenation reaction was started with the addition of 40 psig of H_2 under vortex stirring. We know that H_2 mass-transfer limitations (MTLs) are not introducing a significant error in this work since, for our apparatus with acetone as the solvent and under the vigorous stirring conditions employed, the H_2 MTL limit is $\geq$ca. 25 mmol of H_2/h[26] while the fastest hydrogenation rate we observe is ca. 6.9 mmol of H_2/h, Figure S-1 of the Supporting Information.

Equation 1 shows the stoichiometry for the formation of the Ir(0) nanoclusters, $(2/n)Ir(0)_n$ per 2HCl; the predicted H_2 uptake, Ir(0) formation, and cyclooctane evolution have been quantitatively verified before for our other, closely analogous Ir(0) nanocluster formation reactions.[24] As a control, the expected evolution of 2.0 equiv of cyclooctane (1.0 equiv per Ir) was verified in the present case by quantitative GLC. Note the production of 2.0 equiv of H^+Cl^- (1.0 equiv for each Ir(I) reduced[22b]), eq 1. Confirmation of the presence of 18 ± 5 Å Ir(0) nanoclusters is provided by their visualization by TEM, Figure 1.

$$[(1,5\text{-COD})IrCl]_2 + 5\,H_2 \longrightarrow 2\,\text{cyclooctane} + 2/n\,Ir(0)_n + 2\,H^+ + 2\,Cl^- \quad (1)$$

During the nanocluster formation and concomitant hydrogenation reaction at 22 ± 0.1 °C, NMR and GC/MS analyses show that the neat acetone undergoes 95% conversion in 2 h and has reached 100% conversion in 9 h with a selectivity of 0.95 equiv (95%) 2-propanol and 0.025 equiv (=5% of the converted acetone) of diisopropyl ether (plus 0.025 equiv of water by mass balance), eq 2. The diisopropyl ether is the expected side product from the H^+-catalyzed condensation of two isopropyl alcohol product molecules.[27] Further details regarding the composite reaction stoichiometry due to the consecutive reactions of isopropyl alcohol and then diisopropyl ether formation, plus use of that balanced reaction to calculate properly the product yields, are provided in the Supporting Information.

$$\text{acetone} + H_2 \xrightarrow[\text{nanocluster catalysis}]{Ir(0)_n} \underset{\text{95\%}}{\underset{\text{0.95 equiv.}}{2\text{-propanol}}} + \underset{\text{[0.025 equiv.]}}{\underset{\text{0.025 equiv.}}{\text{diisopropyl ether}}} + H_2O \quad (2)$$

(24) Lin, Y.; Finke, R. G. *J. Am. Chem. Soc.* **1994**, *116*, 8335.
(25) Lin, Y.; Finke, R. G. *Inorg. Chem.* **1994**, *33*, 4891.
(26) (a) Experiments performed with increasing catalyst concentrations, Figure S-2 of the Supporting Information, show the highest observed hydrogenation rate under our specific conditions, apparatus, and vigorous stirring of ca. 25 mmol of H_2/h for a $[(1,5\text{-COD})IrCl]_2$ nanocluster precursor concentration of 1.9 mM; hence, the H_2(gas) to H_2(solution) MTL rate must be $\geq$25 mmol of H_2/h for our current system. For the related system of cyclohexene hydrogenation in acetone as solvent in the same apparatus with vigorous stirring, the H_2 MTL rate is ~17 mmol of H_2/h.[26b] (b) Aiken, J. D., III; Finke, R. G. *J. Am. Chem. Soc.* **1998**, *120*, 9545.

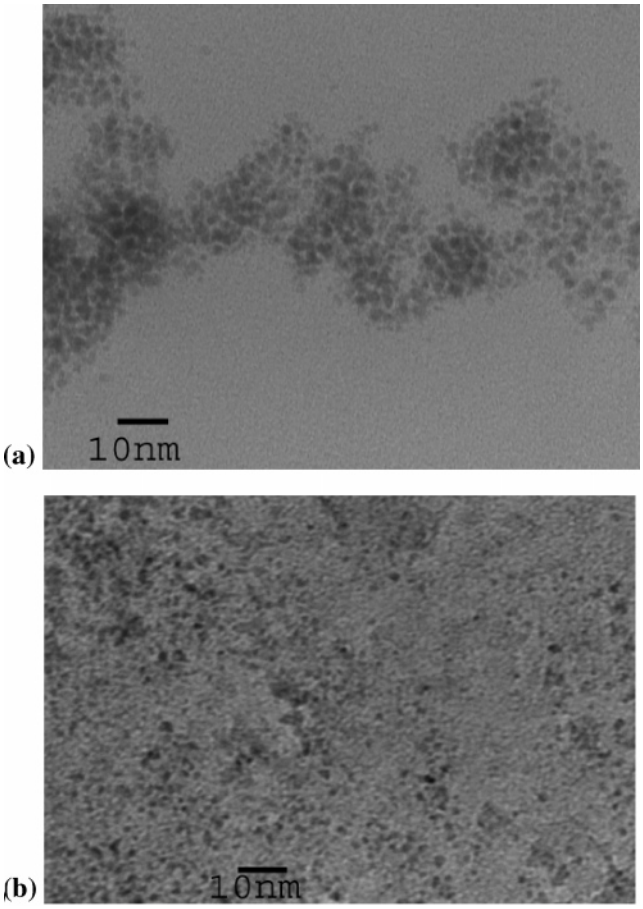

Figure 1. TEM images (340 K) of 18 ± 5 Å Ir(0) nanoclusters formed by the hydrogen reduction of $[(1,5\text{-COD})IrCl]_2$ (3.6 μmol Ir) during the hydrogenation of neat acetone at 22 ± 0.1 °C. (a) Nanoclusters dispersed on a silicon monoxide coated copper grid by dipping it into solution immediately after the hydrogenation (all of which was done under N_2 in a drybox). (b) TEM of a solution of nanoclusters diluted with acetonitrile and then dispersed on a chloroform-cleaned copper grid just before the measurement. The sample was harvested after 0.7 h of hydrogenation (i.e., after ca. 70% conversion of the acetone) since the nanoclusters aggregate to larger particles and ultimately into bulk metal as the hydrogenation proceeds.

Overall, the $(2/n)Ir(0)_n$ plus 2HCl nanocluster system exhibits a record initial activity (TOF(initial, minimum[28]) = 1.92 s^{-1} at 22 °C and 40 psig (= 2.7 atm of H_2)), the highest selectivity (95% 2-propanol) at the highest conversion (100%) for any catalyst reported to date for acetone hydrogenation to 2-propanol. Note that the true TOF may be closer to 11-fold larger

(27) For a review of Williamson ether synthesis, see: Staude, E.; Patat, F. In *The Chemistry of the Ether Linkage*; Patai, R., Ed.; Wiley: New York, 1967; pp 22−46.
(28) (a) The TOFs and TTOs reported herein are those typically reported [TOF = (mol of product)/[(mol of total catalyst loading) s]; TTO = TOF × time = (mol of product)/(mol of total catalyst loading)]. That is, the reported TOFs and TTOs are not corrected for the amount of metal that is on the surface of the catalyst and/or the actual number of active sites. In only one case to date have the quantitative catalyst poisoning studies needed for such active site correction been done for a nanocluster.[28b] In that study, the $P_2W_{15}Nb_3O_{62}^{9-}$ polyoxoanion- and Bu_4N^+-stabilized, 40 ± 6 Å Rh(0) nanoclusters reported elsewhere[28b] have ~31% of the Rh on the surface, but only ~(1.8*X*)% of that total Rh is catalytically active as determined by CS_2 poisoning experiments (where *X* is the number of active Rh sites poisoned by a single CS_2, a working value for which is $X \approx 5$).[28b] Applying those data to the present case for the sake of illustration, *if* this same ~(1.8 × 5) = 9% number is roughly applicable to the present case, results in the reported TOF and TTO values herein being larger by a factor of 100/9 = 11. The resultant values would then be TOF ≈ 1.92 × 11 = 21 s^{-1} and TTO ≈ 188000 × 11 = ~2000000. (b) Hornstein, B. J.; Aiken, J. D., III; Finke, R. G. *Inorg. Chem.* **2002**, *41*, 1625.

due to the amount of active Ir being estimated as ca. 9% from CS_2 poisoning studies on a related Ir nanocluster system,[28] TOF-(true, estimated) $\approx 21\ s^{-1}$.

A control experiment was performed with the original intent of seeing if adding molecular sieves to remove any water present would influence the 5% diisopropyl ether formation. (The water content of the Burdick & Jackson acetone employed is <0.2%, which corresponds to 15.4 equiv of H_2O per iridium used in a standard conditions nanocluster formation and acetone hydrogenation experiment; 1 equiv of water is also formed for every equivalent of diisopropyl ether produced, eq 2.) However, an interesting result was obtained which cannot be explained by an effect of the molecular sieves on the water content but which, instead, implicates a support interaction between the molecular sieves and the $Ir(0)_n$ nanoclusters. Specifically, a standard conditions hydrogenation of acetone at 22 ± 0.1 °C, starting with $[(1,5\text{-COD})IrCl]_2$ (3.6 μmol Ir) in neat acetone (6.7 mmol) with 0.2 g of predried 5 Å molecular sieves added, gave a sigmoidal-shaped curve[29] (Figure S-8 in the Supporting Information). A 100% conversion of acetone to 2-propanol in 6 h is seen, eq 3, with an initial TOF of 0.32 ± 0.02 s^{-1}, as

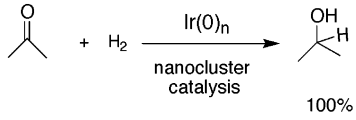

(3)

demonstrated by ^1H and ^{13}C NMR spectra (Figure S-9 in the Supporting Information). Note that the NMR spectra were obtained from the raw hydrogenation product (i.e., without purification); neither spectrum reveals any impurities or side products, such as the previously observed diisopropyl ether (estimated detection limit 1%). The complete conversion of acetone to one product, 2-propanol, at room temperature and ≤3 atm of H_2 in the presence of molecular sieves is an important result. Additional control experiments were performed to confirm that the molecular sieves were not just adsorbing the diisopropyl ether (and thereby obscuring its detection; see the Experimental Section for details). On the basis of kinetic studies of the nanocluster formation in the presence of molecular sieves (Figure S-8 of the Supporting Information), the main effect of adding molecular sieves appears to be on the nanocluster formation reaction (and then subsequent catalysis), presumably by supporting the $Ir(0)_n$ nanoclusters on the molecular sieves.

An additional control experiment also produced an unexpected result: deliberately added water (0.4 wt %, i.e., double the 0.2 wt % in Burdick & Jackson acetone) also led to a 100% selectivity to 2-propanol, the amount of diisopropyl ether side product being reduced to below our detection limit (≤1%). Apparently, added water leads to the precedented[30] hydrolysis of any diisopropyl ether present back to 2-propanol. However, the reaction rate was slowed 2-fold and the catalyst stability reduced, with bulk $Ir(0)_n$ metal precipitating from this control reaction.

Catalyst Lifetime. A catalyst lifetime experiment starting with 0.6 mg of $[(1,5\text{-COD})IrCl]_2$ (i.e., 0.6 mM in Ir) in 3.0 mL of acetone at 22 ± 0.1 °C and at a constant 40 ± 1 psig of H_2 reveals 16400 TTOs of acetone hydrogenation over 32 h before deactivation by aggregation into bulk metal occurs. The *average* TOF during this lifetime is, therefore, 0.14 s^{-1}. Comparison of this TOF to the ca. 4 times faster *initial* TOF provided above makes it clear that the nanoclusters are deactivating as the catalysis proceeds over its 32 h total lifetime. The clear yellow solution turns to brown as the iridium(0) nanoclusters are first formed, followed by the formation of a black, bulk iridium(0) metal precipitate which becomes visible to the naked eye after a few hours along with an eventually clear, colorless (i.e., Ir(0)-free) solution. Hence, the catalytic lifetime is limited to 16400 TTOs in this case, with some of this TTO value being due to bulk Ir(0) metal.

Interestingly, a catalyst lifetime experiment starting with 0.6 mg of $[(1,5\text{-COD})IrCl]_2$ (i.e., 0.6 mM in Ir) in 27 mL of acetone with 0.5 g of 5 Å molecular sieves added, at 22 ± 0.1 °C and at a constant 40 ± 1 psig of H_2, reveals 188000 TTOs of acetone hydrogenation selectively to 100% 2-propanol over 110 h before deactivation by aggregation into bulk metal occurs. Again, due to the formation of bulk metal, this TTO value is an upper limit to the true nanoparticle TTO value.[31] Nevertheless, this is the highest reported value to date that we have been able to find as well as a value which is 115−330-fold higher than those reported in two recent patents (for ketones other than acetone).[38f,g] Again, using the estimate of ∼9% of the total Ir being active, the true TTO (estimated) per active Ir is likely something approaching ∼2000000.[28]

Requirement for Acid and Kinetic Evidence for a $[H^+]^1$ Dependence. To test the hypothesis that the 1 equiv of H^+/Ir(0) formed, eq 1, is crucial for the reaction, the nanocluster formation and acetone hydrogenation reaction were repeated, but now with 1 equiv of added Proton Sponge (1,8-bis-(dimethylamino)naphthalene),[32] a strongly basic (conjugate acid aqueous $pK_a = 12.3$) but weakly coordinating, preferred scavenger of H^+ in such nanocluster syntheses.[22b] As expected, 0.6 mM $[(1,5\text{-COD})IrCl]_2$ (i.e., 1.2 mM in Ir) and 1.2 mM (1 equiv per Ir) Proton Sponge in acetone at 22 ± 0.1 °C exhibits no detectable hydrogen uptake over 8 h. As a control to show that an active catalyst had been formed, the same experiment was performed (0.6 mM $[(1,5\text{-COD})IrCl]_2$ (i.e., 1.2 mM in Ir) and 1.2 mM (1 equiv per Ir) Proton Sponge in acetone at 22 ± 0.1 °C), except with a 1.6 M concentration of the more easily reduced substrate, cyclohexene. The resultant $(2/n)Ir(O)_n$ nanocluster catalyst was quite active, exhibiting the normal, sigmoidal-shaped cyclohexene loss vs time curve[24] (Figure S-5 of the Supporting Information). No acetone hydrogenation was observed in this control experiment as expected (and in which 1 equiv of Proton Sponge was present).

(29) For a mechanism of transition-metal nanocluster formation, consisting of slow, continuous nucleation (A → B, rate constant k_1) and then fast, autocatalytic surface growth (A + B → 2B, rate constant k_2), a mechanism that is proving to be quite general for transition-metal particle formation under reducing conditions, see: (a) Watzky, M. A.; Finke, R. G. *J. Am. Chem. Soc.* **1997**, *119*, 10382 and references therein. (b) Watzky, M. A.; Finke, R. G.; *Chem. Mater.* **1997**, *9*, 3083. (c) Aiken, J. D., III; Finke, R. G. *J. Am. Chem. Soc.* **1998**, *120*, 9545 and references therein to diffusive agglomeration of nanoparticles. (d) Widegren, J. A.; Aiken, J. D., III; Özkar, S.; Finke, R. G. *Chem. Mater.* **2001**, *13*, 312, and references therein.

(30) Adelman, R. L. *J. Am. Chem. Soc.* **1953**, *75*, 2678.

(31) One caveat on the lifetime measurements: when the presence of a bulk metal precipitate is noted, the TTOs given in Table 1 or in the main text are an *upper limit* to the TTOs due to nanoclusters alone and as indicated by placing the TTO number in brackets, [TTOs]. See also Table 1, p 4900, in ref 25 for data showing that any bulk metal present generally has a considerably lower surface area in comparison to that of the nanoclusters and, therefore, a significantly slower rate of hydrogenation than the nanoclusters—a fortunate situation that helps limit (the still nonzero, however) contribution of bulk metal to the observed TTO number.

(32) Proton Sponge: (a) Brzezinski, B.; Schroeder, G.; Grech, E.; Malarski, Z.; Sobczyk, L. *J. Mol. Struct.* **1992**, *274*, 75. (b) Brzezinski, B.; Glowiak, T.; Grech, E.; Malarski, Z.; Sobczyk, L. *J. Chem. Soc., Perkin Trans.* **1991**, *2*, 1643.

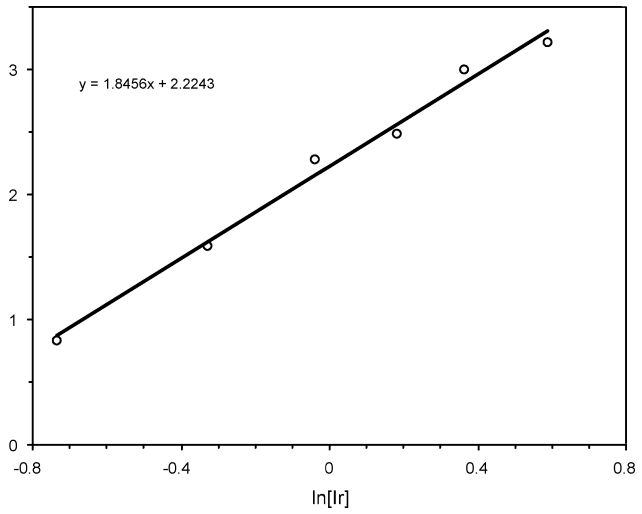

Figure 2. Acetone hydrogenation ln(steady-state rate) vs ln [[(1,5-COD)IrCl]$_2$] for the catalytic hydrogenation of acetone at 22 ± 0.1 °C. The linear plot and slope of 1.9 ± 0.2 reveal an apparent second-order dependence on the initial concentration of [(1,5-COD)IrCl]$_2$, which is, however, as discussed in the text, due to a first-order dependence on $[H]^+$ plus a first-order dependence on [[(1,5-COD)IrCl]$_2$] *plus* their stoichiometric relationship, vide infra.

The acid-assisted nature of the acetone hydrogenation reaction is further, quantitatively supported by initial kinetic studies varying the [(1,5-COD)IrCl]$_2$ from 0.2 to 1.9 mM. An ln/ln plot of the acetone hydrogenation steady-state rate (i.e., the constant rate post the induction period, Figure S2 of the Supporting Information) vs the initial [(1,5-COD)IrCl]$_2$ concentration, Figure 2, is linear and shows a slope of 1.9 ± 0.2. That is, an *apparent* second-order dependence on [(1,5-COD)IrCl]$_2$ concentration is observed, $-\mathrm{d[acetone]}/\mathrm{d}t \propto [[(1,5\text{-COD})\mathrm{IrCl}]_2]^2$.

At first sight the (apparent) second-order dependence upon the initial [(1,5-COD)IrCl]$_2$ concentration is perplexing. However, a bit of reflection reveals what the apparent second-order dependence on the $[\{(1,5\text{-COD})\mathrm{IrCl}\}_2]_{\mathrm{initial}}$ is telling us. To understand this, first one must be aware that the measured hydrogenation rate is the steady-state rate past a short, ca. 0.2 ± 0.1 h induction period, Figure S2. Second, TEM and a cyclooctane evolution experiment[22,29] using GLC confirm that the Ir(0)$_n$ catalyst has fully evolved, in ≤0.6 h, and thus by the time the hydrogenation rate is measured, according to eq 1 so that $[\{(1,5\text{-COD})\mathrm{IrCl}\}_2]_{(\mathrm{initial})} \approx \mathrm{n}\,[\mathrm{Ir}(0)_n]$. Third, we know from the Proton Sponge scavenging experiments that the evolved H^+ (as HCl, eq 1) is crucial for the facile catalysis. It follows, therefore, and as shown in the kinetic derivations in eqs 4−9,

$$-\frac{\mathrm{d[acetone]}}{\mathrm{d}t} = \frac{\mathrm{d[H_2]}}{\mathrm{d}t} = k_{2,\mathrm{obs}}[\mathrm{acetone}]^a[\mathrm{H_2}]^b[\mathrm{Ir}(0)_n]^c[\mathrm{H^+}]^d \quad (4)$$

$$\frac{2}{n}[\mathrm{Ir}(0)_n] = 2[\mathrm{H^+}] \quad (5)$$

$$-\frac{\mathrm{d[acetone]}}{\mathrm{d}t} = \frac{k_{2,\mathrm{obs}}}{n}[\mathrm{acetone}]^a[\mathrm{H_2}]^b[\mathrm{Ir}(0)_n]^{c+1} \quad (\text{for the } d = 1 \text{ case}) \quad (6)$$

that the apparent second-order dependence on the Ir(I) precursor is reflecting the concomitant, stoichiometric production of 1 equiv of H^+ per 1 equiv of Ir(I) reduced, eq 1, and then a first-order dependence on acid, $[H^+]^1$, as well as a first order dependence on the Ir precursor, $[[\{(1,5\text{-COD})\mathrm{IrCl}\}_2]_{\mathrm{initial}}]^1$. Consistent with this interpretation and assuming a general rate law of the form shown in eq 4 for the sake of illustration, eq 5 is just a restatement of the stoichiometry back in eq 1. Substitution of eq 5 into eq 4 followed by the appropriate algebra yields eq 6 (the full details of the kinetic derivations implied by eqs 4−9 are available in the Supporting Information).

Next, one can write the appropriate mass balance equation (7a), which simplifies to eq 7b for the case where the nanocluster formation reaction is fast

$$[\{(1,5\text{-COD})\mathrm{IrCl}\}_2]_{\mathrm{initial}} = [\{(1,5\text{-COD})\mathrm{IrCl}\}_2] + n[\mathrm{Ir}(0)_n] \quad (7a)$$

$$[\{(1,5\text{-COD})\mathrm{IrCl}\}_2]_{\mathrm{initial}} \approx n[\mathrm{Ir}(0)_n] \quad (7b)$$

and most of the initial [(1,5-COD)IrCl]$_2$ is present as Ir(0)$_n$ nanoclusters; that is, eq 7b results when $n[\mathrm{Ir}(0)_n] \gg [\{(1,5\text{-COD})\mathrm{IrCl}\}_2]$. Recall the GLC cyclooctane evolution experiment (vide supra) which demonstrated that the Ir(0)$_n$ catalyst does, indeed, evolve in ≤0.6 h according to eq 1; that is, the simplification of eq 7a to eq 7b has experimental support. Inserting eq 7b into eq 6, then, yields the desired eqs 8 and 9.

$$-\frac{\mathrm{d[acetone]}}{\mathrm{d}t} = \frac{\mathrm{d[H_2]}}{\mathrm{d}t} = \frac{k_{2,\mathrm{obs}}}{n}[\mathrm{acetone}]^a[\mathrm{H_2}]^b[[\{1,5\text{-CODIrCl}\}_2]_{\mathrm{initial}}]^{c+1} \quad (8)$$

$$-\frac{\mathrm{d[acetone]}}{\mathrm{d}t} = \frac{\mathrm{d[H_2]}}{\mathrm{d}t} \propto [[\{1,5\text{-CODIrCl}\}_2]_{\mathrm{initial}}]^{c+1} \quad (9)$$

From eq 8, it is apparent if the reaction is first-order in [(1,5-COD)IrCl]$_2$ (i.e., for $c = 1$ and with fast nanocluster formation so that eq 7b is in effect), then the reaction will appear to be second-order in [(1,5-COD)IrCl]$_2$, eq 9, as is observed experimentally.

In short and although a full kinetic study remains to be performed, the key point of these initial kinetic as well as added Proton Sponge studies is that *H^+ is essential*; that is, the present Ir(0) nanocluster catalyzed acetone hydrogenation reaction is strongly *acid-assisted*.

Demonstration of Reproducible Reaction Rates. Because Bradley[33] has shown that the uncontrolled production (and loss) of volatile H^+Cl^- in nanoparticle synthesis reactions yields nanoparticles with catalytic rates variable by up to ±670%, it was important for us to establish if our catalysis is reproducible or not. We expected that it would be, since our system is a closed system (a sealed Fischer−Porter pressure bottle) while Bradley's was by design an open system, so that the volatile HCl could be lost. However, it was still important to test experimentally the reproducibility of our system.

(33) (a) The difference between nanoclusters and the historically better known nanocolloids[33] is convincingly illustrated by Bradley's seminal paper showing that irreproducibility in the colloid's composition of surface-bound Cl^-/H^+Cl^-, the latter being the byproduct of the nanocluster formation reaction, is the origin of the up to 670% irreproducibility in the rate of catalysis by Pt/PVP/H^+Cl^- nanocolloids: Köhler, J. U.; Bradley, J. S. *Catal. Lett.* **1997**, *45*, 203. (b) Five-fold (i.e., 500%) rate variations are seen for the photoreduction of CO_2 catalyzed by a series of 10 different batches of the Pd colloids: Willner, I.; Mandler, D. *J. Am. Chem. Soc.* **1989**, *111*, 1330.

In four repeat acetone hydrogenations under standard conditions, we find a reproducible rate of 6.9 ± 0.2 mmol of H_2/h (±3%) for the acid-assisted, iridium(0) nanocluster catalyzed hydrogenation of acetone (and over the use of several batches of the commercially available, well-known, pure precatalyst $[(1,5\text{-COD})IrCl]_2$, to answer the query of a reviewer). The reasons that our nanocluster catalysis is 230-fold more reproducible than Bradley's important, illustrative system are (i) our closed, Fischer−Porter bottle reaction system noted above which retains all the volatile H^+Cl^-, (ii) our use of a structurally and compositionally well characterized precursor, a known requirement for reproducible nanocluster syntheses and catalytic rates,[18c] and (iii) the fact that we carry out the reaction under exactly the same conditions each time (the same catalyst and substrate concentrations, temperature, pressure, and stirring rate, for example; see the Experimental Section for further details).

Attempted Extension of the Catalytic Lifetime of the Iridium(0) Nanoclusters by Using the Polar Solvent Propylene Carbonate To Extend the Nanocluster Stability. Because we[34] and others[35] have shown that the polar, noncoordinating solvent propylene carbonate is as good as any presently available to improve the lifetime, isolabilty, and stability of anionically (e.g., Cl^-) stabilized transition-metal nanoclusters, experiments examining the hydrogenation of acetone in propylene carbonate were undertaken (i.e., rather than in neat acetone as has been done up to this point). The key result of these experiments (which are descried in detail in the Supporting Information) is that a more stable, clear-brown solution of 21 ± 3 Å nanoclusters (Figure S-3 in the Supporting Information) is produced which remains stable and catalytically active at room temperature under N_2 for even 3−4 weeks after the initial acetone hydrogenation reaction. However, the maximum rate of hydrogenation (≤2 mmol of H_2/h) is 3.5-fold slower than that in neat acetone (6.9 ± 0.2 mmol of H_2/h). Furthermore, a catalyst lifetime experiment starting with 0.6 mg of $[(1,5\text{-COD})IrCl]_2$ (i.e., 0.6 mM in Ir) and 3.0 mL of acetone in 2.5 mL of propylene carbonate at 22 ± 0.1 °C and 40 ± 1 psig of H_2 shows that the Ir(0) nanoclusters in propylene carbonate afford only 4800 TTOs of acid-assisted acetone hydrogenation over 122 h before deactivation by aggregation into bulk metal. This catalytic lifetime in propylene carbonate is 3.4-fold lower, despite the 3.8-fold longer reaction time, in comparison to the TTOs observed for the superior, neat acetone system. The catalysis of neat acetone hydrogenation is, therefore, an important as well as "green"[43] component of the present invention ("green" since cosolvent is not only not needed,[43] it is actually a disadvantage).

Evidence Regarding the Catalytic Mechanism Using D-Labeled Acetone. Given that H^+ is a requirement in our acetone reduction system, a reasonable question is whether the enol of acetone is the actual species being reduced. The prediction from the literature here is clear: a direct 1,2 addition of H_2 (D_2) across the ketone is expected, with the enolization mechanism becoming important only at higher temperatures.[1] To test the mechanism, D-labeled acetone-d_6 and H_2 were employed. In an experiment starting with 0.6 mM $[(1,5\text{-COD})IrCl]_2$ (i.e., 1.2 mM in Ir) in deuterated acetone, $(CD_3)_2CO$, at 22 ± 0.1 °C, the same product distribution is obtained as before, again with 100% conversion: after 7.5 h, NMR and GLC/MS analyses show that the deuterated acetone is completely converted to 2-propan-*1,1,1,3,3,3*-d_6-ol (95%) plus diisopropyl ether and, by mass balance, water (0.025 equiv each). Significantly, the MS analysis is definitive in showing that both the 2-propanol and diisopropyl ether have all the D atoms in the methyl groups, eq 10, and as shown by the data supplied in the

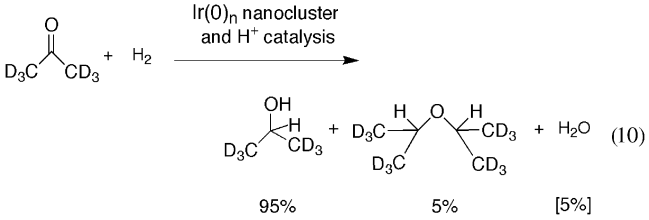

(10)

Experimental Section (Complete Hydrogenation of Deuterated Acetone). The enol of acetone is *not* involved in the Ir(0) nanocluster mechanism under our catalytic conditions.[36] A literature study of a C-supported Ru catalyst has shown that a mixture of 2-propanol and deuterated acetone also gives 2-propan-*1,1,1,3,3,3*-d_6-ol and acetone, with no enolization.[37]

Proposed Minimum Mechanism for the Acid-Assisted Catalytic Hydrogenation of Acetone. There is excellent product, structural, kinetic, mechanistic, and computational work in the literature of homogeneous, organometallic complex catalysis of ketone and other polar group hydrogenations (i.e., C═N, imines) from the groups of Vos, Harman/Taube, Eisenberg, Bullock, Norton, Casey, and Noyori.[15,38,39] The essence of that combined literature that is relevant to the present work is (i) that "ionic hydrogenations" of polar groups are facile when a M−H and H^+ component are both present, and (ii) that mechanisms ranging from those involving a prior protonation of acetone, to a concerted M−H and H^+ addition to ketones in a 1,2 fashion, are well documented.

Given the complex, always challenging mechanistic issue of the timing of steps where two or more species are involved (i.e., $M-H^-/H^+$ in the present case), the most plausible, deliberately minimal (Occam's razor) mechanism in our system can be written concisely as shown in eqs 11a and 11b.

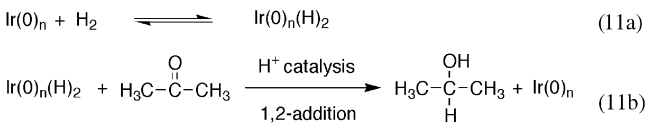

(11a)

(11b)

This deliberately brief mechanistic scheme is consistent with and supported by the experiments using D-labeled acetone, the kinetic studies implicating a first-order dependence on both the [Ir] and $[H^+]$, as well as the above-noted, excellent precedent

(34) Hornstein, B. J.; Finke, R. G. *Chem. Mater.* **2003**, *15*, 899−909.
(35) Reetz, M. T.; Lohmer, G. *J. Chem. Soc., Chem. Commun.* **1996**, 1921−1922.
(36) Our results require that the enolization of acetone with *dry* H^+Cl^- is slow under our conditions given the D-isotope is involved, as otherwise the following reversible reaction would have scrambled D^+/H^+ in the acetone methyl groups: $CD_3C(O)CD_3 + H^+ \rightarrow CD_2{=}C(OH)CD_3 + D^+$, then $CD_2{=}C(OH)CD_3 + H^+ \rightarrow HCD_2C(O)CD_3 + H^+$.
(37) Yamashita, M.; Kawamura, T.; Suzuki, M.; Saito, M. *Bull. Chem. Soc. Jpn.* **1991**, *64*, 272.
(38) (a) Bullock, R. M.; Song, J.-S. *J. Am. Chem. Soc.* **1994**, *116*, 8602. (b) Bullock, R. M.; Luan, L.; Song, J.-S. *J. Org. Chem.* **1995**, *60*, 7170. (c) Bullock, R. M.; Voges, M. H. *J. Am. Chem. Soc.* **2000**, *122*, 12594. (d) Voges, M. H.; Bullock, R. M. *J. Chem. Soc., Dalton Trans.* **2002**, 759. (e) Song, J.-S.; Szalda, D. J.; Bullock, R. M. *Organometallics* **2001**, *20*, 3337. (f) Bullock, M. R.; Schlaf, M.; Hauptman, E. M. US Patent 6,462,206, Oct 8, 2002. (g) Bullock, M. R.; Kimmich, B. F.; Fagan, P. J.; Hauptman, E. M. US Patent 6,613,923, Sept 2, 2003.

from the mechanistic organometallic literature. That extant literature of ketone and other, polar functional group hydrogenations[15,38,39] (a) effectively predicts that the mechanism of nanocluster catalysis in the present work should be H^+-assisted—as it is; and (b) therefore offers strong support for the findings herein of H^+-assisted acetone hydrogenation. Moreover, the pK_a values of H^+Cl^- and protonated acetone, $(CH_3)_2C{=}O{-}H^+$, are similar (p$K_a \approx -7$),[40] indicating that a substantial fraction of the acetone should be protonated under our (highly acidic) reaction conditions (and assuming that sizable differential solvent effects on these pK_a values are not present). The reader interested is referred to the cited literature[15,38,39] for further details of the most probable, additional mechanistic steps underlying the present Ir−H- and H^+-assisted acetone hydrogenation.

Summary

The main findings of this work, including the limitations, as well as the implications or predictions of our findings, can be summarized as follows.

(1) A system for the room temperature, acid-assisted hydrogenation of acetone by Ir(0) nanoclusters has been developed, one which provides exceptional (record) activity, up to 100% selectivity at 100% conversion, and up to 188000 TTO catalytic lifetime. The system is easily and reproducibly prepared from commercially available $[(1,5\text{-COD})IrCl]_2$ and H_2; the use of neat acetone, and the 1 equiv of H^+Cl^- generated per Ir reduced that is retained in the closed system, is an important component of the present discovery.

(2) The addition of molecular sieves yields an enhanced catalytic lifetime of 188000 TTOs, perhaps because the nanoclusters become supported on the molecular sieves, thereby reducing the nanocluster's tendency to agglomerate. Use of the polar, nanocluster-stabilizing solvent propylene carbonate did yield more stable, albeit less catalytically active, Ir(0) nanoclusters. The current Achilles heel of this system then, as with most soluble nanoclusters, is their limited catalytic lifetime and instability at raised temperatures.[18,19] The present system is not, for this reason, expected to have any impact on the acetone to 2-propanol heat pump problem, since temperatures in the 200 °C range are preferred there.[3] However, the factors determining the stability of modern transition-metal nanoclusters are only just now becoming better understood,[22] so that improvements in this area can be anticipated (and are beginning to appear[35,41]). And simply supporting the nanoclusters, for example, by performing the reaction with the mesoporous silica SBA-15 present, may lead to improved catalysis.[42]

(3) The most probable mechanism of these ionic hydrogenations[38,39] is that anticipated from the literature,[1,38,39] a 1,2 addition of the expected[38,39] $M{-}H/H^+$ components across the polar C═O bond. Strong support for this minimal mechanism is provided by labeling studies using acetone-d_6, kinetic studies revealing a $[H^+]^1$ dependence, complete inhibition experiments using Proton Sponge which demonstrate the requirement for acid, and the excellent mechanistic precedent in the organometallic literature.[38,39]

(4) The present system is "relatively green" in its environmental impact in that it satisfies 7 of the 12 proposed principles of green chemistry detailed elsewhere[43] including that (i) it is 100% selective and minimizes any byproducts or waste, (ii) it exhibits atom economy by incorporating all the reactants into the products, (iii) it is solventless (i.e., uses neat acetone as the substrate/solvent), (iv) it has relatively low energy requirements due to its room temperature and ≤3 atm pressure conditions, (v) it is catalytic not stoichiometric, (vi) it does not use any derivatization (blocking or protecting/deprotecting groups; in the present case this is effectively a restatement of the fact that the reaction is accomplished catalytically), and (vii) real-time monitoring is easy by following the H_2 pressure loss or the products by GLC or ^{1}H NMR, for example.

Some implications or as of yet untested predictions of this work are also apparent, as listed below.

(i) The extension to other, polar functional group selective reductions is expected, since as McGee and Norton have noted[39d] "ionic hydrogenations lend themselves to selecting polar C═X bonds (for reduction) over C═C bonds". Imine, C═N reductions via $M{-}H/H^+$ ionic hydrogenations are of course already known,[15f,39d,e] and we have already observed CH_3CN reduction to $CH_3CH_2NH_2$ by our Ir(0)/HCl catalyst system.[21] Also of interest, but not established by this first report, are the scope of higher ketones, $R{-}C(O){-}R'$, that can (or cannot) be reduced, and the functionality that can (or cannot) be tolerated in more complex C═X bond reductions (i.e., acid-sensitive groups are expected to prove problematic).

(ii) The present system should be immediately extendable to Rh(0)/HCl nanoclusters since we have shown that nanoclusters of other metals are obtained from analogous, commercially available, $[(1,5\text{-COD})RhCl]_2$ and $[(1,5\text{-COD})MCl_2]$ systems (M(II) = Pd, Pt, Ru) if appropriate conditions are employed in the different cases.[44] Studies are in progress to see if the general reactivity trend found for γ-Al_2O_3-supported metals[12] of Pt > Tc ≈ Rh > Pd > Ru > Ni ≈ Re > Co is the same or different for nanocluster catalysts.[44]

(iii) Last, the present results may be of at least general interest to other problems, notably the need for H^+X^--tolerant, expanded lifetime catalysts for $C{-}X + H_2 \rightarrow C{-}H + H^+X^-$ hydrodehalogenation catalysis important in environmental remedia-

(39) (a) Tooley, P. S.; Ovalles, C.; Kao, S. C.; Darensbourg, D. J.; Darensbourg, M. Y. *J. Am. Chem. Soc.* **1986**, *108*, 5465. (b) Song, J.-S.; Szalda, D. J.; Bullock, R. M.; Lawrie, C. J. C.; Rodkin, M. A.; Norton, J. R., *Angew. Chem., Int. Ed. Engl.* **1992**, *31*, 1233. (c) Smith, K.-T.; Norton, J. R.; Tilset, M. *Organometallics* **1996**, *15*, 4515. (d) McGee, M. P.; Norton, J. R. *J. Am. Chem. Soc.* **2001**, *123*, 1778. (e) Casey, C. P.; Singer, S. W.; Powell, D. R.; Hayashi, R. K.; Kavana, M. *J. Am. Chem. Soc.* **2001**, *123*, 1090.

(40) Gordon, A. J.; Ford, R. A. *The Chemist's Companion, A Handbook of Practical Data, Techniques and References*; Wiley-Interscience: New York, 1972; p 60.

(41) (a) Aiken, J. D., III; Finke, R. G. *J. Am. Chem. Soc.* **1999**, *121*, 8803. Note that the true active-site-corrected TOF and TTO for the polyoxoanion- and Bu_4N^+-stabilized nanoclusters in that study, based on CS_2 poisoning studies (the first kind for a nanocluster system), are TOF ≈ 380900 h^{-1} and TTO = 2142000.[34] (b) Li, Y.; El-Sayed, M. A. *J. Phys. Chem. B* **2001**, *105*, 8938. (c) Narayanan, R.; El-Sayed, M. A. *J. Am. Chem. Soc.* **2003**, *125*, 8340. (d) Interesting early work, which provides high TOF and TTO, but in an ill-characterized colloidal[33] system where the true catalyst is not known for certain, is Beller, M.; Fischer, H.; Kühlein, K.; Reisinger, C.-P.; Herrmann, W. A. *J. Organomet. Chem.* **1996**, *520*, 257.

(42) The catalytic activity of SBA-15-supported Ir(0) nanoclusters for acetone hydrogenation was tested in an initial experiment as follows: a standard conditions acetone hydrogenation was performed by starting with 0.6 mM $[(1,5\text{-COD})IrCl]_2$ in acetone (3.0 mL) at 22.0 ± 0.1 °C and 40 psig of H_2 in the presence of SBA-15 (50 mg, corresponding to 1.4% (by weight) Ir on the support); we thank Prof. T. D. Tilley at the University of California at Berkeley for providing us the sample of SBA-15. The resulting Ir(0) nanoclusters/H^+Cl^-/SBA-15 system converted neat acetone to 95% 2-propanol and diisopropyl ether plus water by mass balance (0.025 equiv each), at 12.1 ± 2 mmol of H_2/h, ca. 2-fold faster than in the absence of SBA-15.

(43) Poliakoff, M.; Fitzpatrick, J. M.; Farren, T. R.; Anastas, P. T. *Science* **2002**, *297*, 807.

(44) Finney, E. E.; Özkar, S.; Finke, R. G. Unpublished results and experiments in progress.

tion.[45] Sonochemically prepared Mo_2C and W_2C catalysts, for example, operate at 225−325 °C with catalyst half-lives as long as 600 h and catalytic activities of 10^{17}−10^{20} molecules·g^{-1}·s^{-1},[46] so that nanoclusters of greatly enhanced stability would be needed before any such application would become possible. Other possible applications can be imagined as well.[47]

Experimental Section

Materials. All commercially obtained compounds were used as received unless indicated otherwise: acetone was purchased from Burdick & Jackson (water content <0.2%) and was purged with argon and transferred into a nitrogen atmospheres drybox before use. It is known that the source and H_2O content of the acetone both matter for reproducible nanocluster syntheses.[24,25] Propylene carbonate (Aldrich, 99.7%, anhydrous, water content <0.002%, packaged under N_2) was transferred into the drybox and used as received. Cyclohexene (Aldrich, 99%) was purified by distillation over sodium under argon and stored in the drybox. Deuterated NMR solvents $CDCl_3$, $(CD_3)_2CO$, and CD_2Cl_2 (Cambridge Isotope Laboratories) were received in 1 mL glass ampules which were transferred into a Vacuum Atmospheres drybox for NMR sample preparations therein.

Analytical Procedures. Unless otherwise reported all reaction solutions were prepared under oxygen- and moisture-free conditions using a Vacuum Atmospheres nitrogen drybox (<1 ppm O_2). High-resolution solution NMR spectra were taken on a Varian INOVA-300 instrument (^{1}H, 300.115 MHz; ^{13}C, 75.472 MHz; ^{31}P, 121.489 MHz). Gas chromatography−mass spectrometry (GC−MS) was performed using a Hewlett-Packard 5890 series II GC instrument with an MSD 5970 B. The GC instrument was equipped with a 30 m (0.25 mm i.d., 0.25 μm film thickness) Supelco SPB-1 column. The ionizing voltage was 70 eV. The GC parameters were as follows: initial temperature, 50 °C; initial time, 3 min; solvent delay, 2 min; temperature ramp, 10 °C/min; final temperature, 270 °C; final time, 5 min; injector port temperature, 280 °C; detector temperature, 290 °C; injection volume, 0.1 μL. The mass marker calibration of the GC−MS instrument was performed using perfluorotributylamine.

Transmission Electron Microscopy (TEM). TEM analyses were performed as before at the University of Oregon with the expert assistance of Dr. Eric Schabtach or JoAn Hudson, using the sample preparation procedure and Philips CM-12 TEM instrument with a 70 μm lens operating at 100 kV and with a 2.0 Å point-to-point resolution, as described in detail previously.[22,24,25]

Sample Preparation for TEM. The solutions used for the TEM analysis were prepared by a standard conditions hydrogenation of acetone (0.5 mL, 6.7 mmol) starting with 1.2 mg of $[(1,5\text{-COD})IrCl]_2$ (3.6 μmol of Ir) either in neat acetone or in propylene carbonate (2.5 mL) at 22.0 ± 0.1 °C. In neat acetone the TEM sample was harvested from the solution after 0.7 h of hydrogenation because the nanoclusters aggregate to larger particles and ultimately into bulk metal as the hydrogenation proceeds. In propylene carbonate the TEM sample was harvested from the solution after 11 h, a time when cyclooctane evolution experiments show that all the $[(1,5\text{-COD})IrCl]_2$ has been converted to $Ir(0)_n$ nanoclusters. (This is imporant, since it has recently been shown that TEM of samples still containing organometallic precursors can lead to TEM-induced nanoparticle formation, thereby introducing artifacts into the TEM analysis.[48]) After the hydrogenation was stopped, the F−P bottle was detached from the hydrogenation line via its quick connects and brought back into the drybox, and its solution was quantitatively transferred with a disposable polyethylene pipet into a clean, 5 mL screw-capped glass vial. The vial was sealed and sent to the University of Oregon for TEM investigation. There, one drop of the sample solution was added to 1 mL of acetonitrile, in air, just before a TEM image was obtained, to yield a clear amber, homogeneous solution (in general, no bulk metal was visible by the naked eye at any time unless otherwise indicated). A drop of this solution was then dispersed on a chloroform-cleaned, carbon-coated Cu TEM grid.

Particle Size Measurements. Particle size analysis was performed using the public domain NIH Image 1.62 program developed at the U.S. National Institutes of Health, available on the Internet at http://rsb.info.nih.gov/nih-image/, and as described in detail elsewhere.[49]

Hydrogenations. All the nanocluster formation and hydrogenation reactions were carried out on the previously described custom-built pressurized hydrogenation apparatus.[22,25,29]

Curve Fits of the Hydrogen Uptake Data and Data Handling. Curve-fitting of the H_2 pressure (or, equivalently, the cyclohexene, or acetone) vs time data was performed, as described previously in detail,[22,25,29] using the software package Microcal Origin 3.5.4, which is a nonlinear regression subroutine (RLIN) and uses a modified Levenberg−Macquard algorithm.[50]

General Procedure for Nanocluster Formation and Acetone Hydrogenation (Standard Conditions) Experiments. These were generally done by our established protocol, but with acetone as the hydrogenation substrate.[25,29a] Details are given in the Supporting Information.

Acetone Hydrogenation Experiments. Additional Details. In a 2 dram glass vial, 1.2 mg (3.6 μmol of Ir) of the precatalyst $[(1,5\text{-COD})IrCl]_2$ was weighed and dissolved in 0.5 mL (6.7 mmol) of acetone, added with a 1.0 mL gastight syringe, to yield a clear, yellow solution. The solution was then transferred via a disposable polyethylene pipet into a new 22 × 175 mm Pyrex culture tube containing a new 5/16 × 5/8 in. Teflon-coated stir bar. The culture tube was then sealed inside the F−P pressure bottle and brought outside the drybox, and the hydrogenation was carried out exactly as described in the previous section and its Supporting Information. The hydrogenation was continued until the complete conversion of acetone was observed as judged by monitoring the hydrogen uptake (Figure S-1 in the Supporting Information). When no more hydrogen uptake was observed, the experiment was stopped and the F−P bottle was sealed, disconnected

(45) A few lead references to the more extensive area of C−X bond hydrodehalogenation/remediation: (a) Richmond, T. G. *Top. Organomet. Chem.* **1999**, *3*, 243−269. (b) Schrick, B.; Blough, J. L.; Jones, A. D.; Mallouk, T. E. *Chem. Mater.* **2002**, *14*, 5140−5147. (c) Oxley, J. D.; Suslick, K. S. Presented at the 225th ACS National Meeting, New Orleans, LA, 2003; Paper INOR-072. See also: Oxley, J. D.; Mdleleni, M.; Suslick, K. S. Presented at the 224th ACS National Meeting, Boston, MA, 2002; Paper INOR-100. (d) Yu, H.; Kennedy, E. M.; Azhar U., M.; Dlugogorski, B. Z. *Appl. Catal., B* **2003**, *44* (3), 253−261. (e) Park, C.; Menini, C.; Valverde, J. L.; Keane, M. A. *J. Catal* **2002**, *211* (2), 451−463.

(46) (a) Oxley, J. D.; Mdleleni, M. M.; Suslick, K. S. *Catal. Today* **2004**, *88* (3−4), 139−151. (b) Sonochemical preparation of the metal carbides: Suslick, K. S.; Hyeon, Fang, M. *Chem. Mater.* **1996**, *8*, 2127.

(47) (a) Benzene is commercially converted to phenol, plus the coproduct acetone, by a current process that involves the alkylation of benzene with propene to give cumene, cumene autoxidation to cumene hydroperoxide, and then acid-catalyzed decomposition of cumene hydroperoxide to phenol and acetone.[47b] A problem with this coproduct process is that the demand for phenol is outstripping the demand for acetone, and for such a large volume of commodity chemicals, even a small difference in demand leads to a glut of the coproduct in smaller demand, in this case acetone. While direct routes for benzene to phenol using, for example, N_2O and Fe catalysts are being developed,[47c] one can at least conceive of a route that recycles the acetone by its H_2 reduction to 2-propanol, and then dehydration of the 2-propanol to propene which could be reused. This would be in essence a H_2/O_2 process, analogous to the one that is being explored for other oxygenations (e.g., propene to propylene oxide) but using Au/TiO_2 catalysts.[47d] However, at present such a recycled acetone and propene process is not of commercial interest, it appears, due to the fact that the acetone can be sold as long as the price is low enough. This situation could change in the future, however, making a process that recycles some of the acetone of future interest. (b) *Kirk Othmer Encyclopedia of Chemical Technology*, 4th ed.; Wiley: New York, 1996; Vol. 18, pp 592−602. (c) Panov, G. I.; Uriarte, A. K.; Rodkin, M. A.; Sobolev, V. I. *Catal. Today* **1998**, *41*, 365 and references therein, notably to the Solutia process for the direct conversion of benzene to phenol using N_2O as the oxidant. (d) Hayashi, T.; Tanaka, K.; Haruta, M. J. *Catalysis* **1998**, 178, 566 and subsequent papers in the area of Au/TiO_2-catalyzed H_2/O_2 epoxidation of propene.

(48) (a) Jaska, C. A.; Manners, I. *J. Am. Chem. Soc.* **2004**, *126*, 9776. (b) Hagen, C. M.; Widegren, J. A.; Maitlis, P. M.; Finke, R. G. Is It Homogeneous or Heterogeneous Catalysis? Compelling Evidence for Both Types of Catalysts Derived from $[Rh(\eta^5\text{-}C_5Me_5)Cl_2]_2$ as a Function of Temperature and Hydrogen Pressure. *J. Am. Chem. Soc.* **2005**, in press.

(49) Woehrle, G. H.; Hutchison, J. E.; Özkar, S.; Finke, R. G. Computer-Based, Statistically Valid Analysis of Nanoparticle Transmission Electron Microscopy Data Using a Public Domain Image-Processing Program, Image. *Mater. Charact.*, submitted for publication.

(50) Press, W. H.; Flannery, B. P.; Teukolsky, S. A.; Vetterling, W. T. *Numerical Recipes*; Cambridge University: Cambridge, U.K., 1989.

from the hydrogenation line, and transferred back into the drybox. After the H_2 pressure was released, a 9 in. glass Pasteur pipet was used to withdraw a ca. 0.05 mL aliquot from the culture tube. This reaction solution aliquot was then added to 1 g of $CDCl_3$ in an individual glass ampule, mixed under agitation using the Pasteur pipet, and then transferred into an NMR sample tube which was subsequently sealed and then brought out of the drybox. The ^{1}H NMR spectrum of this solution showed that the acetone is completely converted to 2-propanol (0.95 equiv, δ (ppm) 4.01 heptet, 1.92 broad, 1.20 doublet) and diisopropyl ether (0.025 equiv, δ (ppm) 3.64 heptet, 1.12 doublet). The ^{13}C NMR spectrum verified the product identifications (δ (ppm) 64.57, 25.51 for 2-propanol, 68.60, 23.05 for diisopropyl ether). Another 0.1 mL aliquot of the solution in a culture tube was used for GC−MS analysis, which showed only 2-propanol, $(CH_3)_2CHOH$, as the major product and diisopropyl ether, $(CH_3)_2CHOCH(CH_3)_2$, as the minor product. The comparison of the fragmentation pattern in the MS spectra with those of the library spectra unambiguously identifies the major and minor products. Neither NMR nor GC−MS showed the presence of detectable, unreacted acetone. (The residual acetone detection limit is estimated as ≤1%.)

Complete Hydrogenation of Acetone Selectively to 2-Propanol. The same hydrogenation experiment as in the previous section was carried out, except that 0.2 g of predried 5 Å molecular sieves were added. An acetone loss vs time plot (Figure S-8 in the Supporting Information) exhibits a sigmoidal shape with a short induction period of 0.5 ± 0.1 h, after which a linear hydrogen uptake of 4.1 ± 0.2 mmol of H_2/h is observed. The sigmoidal curve is well-fit by the A → B nucleation (rate constant k_1) and then A + B → 2B autocatalytic surface-growth (rate constant k_2) mechanism for nanocluster formation as first detailed elsewhere[28] with $k_1 = 0.066 \pm 0.003$ h^{-1} and $k_2 = (1.3 \pm 0.1) \times 10^3$ M^{-1}h^{-1}. The ^{1}H and ^{13}C NMR spectra of the solution after reaction show 2-propanol as the only detectable product (Figure S-9 in the Supporting Information); GC−MS also is unable to detect any unreacted acetone or side products (estimated detection limits ≤1%).

Complete Hydrogenation of Deuterated Acetone. The same hydrogenation experiment as in the previous section, but with deuterated acetone, was carried out to obtain mechanistic insight into the hydrogenation reaction (Figure S-6 in the Supporting Information). The ^{1}H NMR spectrum of this solution showed that the deuterated acetone is completely converted to propan-*1,1,1,3,3,3-d*$_6$-2-ol (0.95 equiv) or diisoropyl ether (0.025 equiv); in both cases no CH_3 signal was observed. The ^{13}C{^{1}H} NMR spectrum gives a singlet for the CH carbon and a heptet with $J(^{13}C-^2D) = 77.4$ Hz for the CH_3 group, while the coupled ^{13}C NMR spectrum shows additional splitting only for the CH signal to a doublet, $J(^{13}C-^1H) = 140$ Hz. These results verify that the 2-propanol product carries the deuterium atoms only on the terminal carbons and the hydrogen only on the second carbon and the hydroxyl, OH, group. Another 0.1 mL aliquot of the solution in a culture tube was used for GC−MS analysis; only propan-*1,1,1,3,3,3-d*$_6$-2-ol, $(CD_3)_2$-CHOH, as the major product, and the minor product diisopropyl ether, $(CD_3)_2CHOCH(CD_3)_2$, were observed. The match of the observed fragmentations with the isotopic mass distribution from the library spectra unambiguously demonstrates that both products have D atoms only in the methyl groups. Notably, for the $(CD_3)_2CHOH$ ($m/z = 66$ = [M]) major product one observes a peak at $m/z = 65$ assignable to [M − H] = $(CD_3)_2C{=}OH^+$ and a base (100%) peak at $m/z = 48$ assignable to [M − CD_3] = 48; the $m/z = 18$ peak for CD_3^+ was also observed). For the minor product, the molecular ion peak (M^+) at $m/z = 114$ and a CD_3 (M − 18) fragment at $m/z = 96$ are as expected for $(CD_3)_2CH-O-CH(CD_3)_2$. By comparison, in the case of the minor product, $(CH_3)_2CH-O-CH(CH_3)_2$, obtained from the hydrogenation of undeuterated acetone the M^+ and M − CH_3^+ fragment peaks are at $m/z = 102$ and $m/z = 87$, respectively, also as expected. Overall, the comparison of the mass spectra and their fragmentation patterns with those of the instrument's library spectra (WILEY6N.L) and also those available in the literature[51] thereby unambiguously identifies the major $(CD_3)_2CHOH$, and minor $(CD_3)_2CH-O-CH(CD_3)_2$, products. Neither NMR nor GC−MS showed the presence of any detectable unreacted acetone (i.e., ≤1%).

Catalyst Lifetime Experiments. The catalyst lifetime experiments were performed by following our established protocol, but with acetone as the hydrogenation substrate.[25] Details are given in the Supporting Information.

Control Experiment of Acetone Hydrogenation Starting with [(1,5-COD)IrCl]$_2$ Plus 1 equiv of Proton Sponge. The same acetone hydrogenation experiment as in the standard conditions hydrogenation, but with 1 equiv of added Proton Sponge,[22b] was carried out to test the role of protons in the catalytic hydrogenation of acetone. After 8 h, there was no detectable hydrogen uptake as monitored by measuring the hydrogen pressure.

Control Experiments of Cyclohexene Hydrogenation (Standard Conditions) Starting with [(1,5-COD)IrCl]$_2$ Plus Cyclohexene in the Absence or Presence of 1 equiv of Proton Sponge. Two standard conditions cyclohexene hydrogenation experiments were performed starting with 1.2 mg (3.6 μmol) of [(1,5-COD)IrCl]$_2$ plus 0.5 mL (4.9 mmol) of cyclohexene in 2.5 mL of acetone without or with 1 equiv of Proton Sponge. In the experiment without Proton Sponge, the fast cyclohexene hydrogenation was followed by the slower hydrogenation of acetone (Figure S-4 in the Supporting Information), while in the experiment with Proton Sponge there was no detectable hydrogen uptake after the cyclohexene hydrogenation (Figure S-5 in the Supporting Information).

Control Experiments with Added Molecular Sieves or Added H_2O. Control experiments were performed addressing the effect of added molecular sieves or water on the reaction's selectivity (eq 2). The first control experiment was performed by adding a known amount of water to acetone to address the following question: Does a 2-fold increase in the amount of water affect the catalytic activity or the product selectivity of the system? A standard conditions hydrogenation of acetone starting with [(1,5-COD)IrCl]$_2$ (3.6 μmol of Ir) in neat acetone (6.7 mmol) containing 0.4% water (recall that the Burdick & Jackson acetone contains <0.2% water) at 22 ± 0.1 °C completely (100%) converts acetone to 2-propanol as the sole product in 11 h (eq 3, main text) as determined by ^{1}H and ^{13}C NMR spectra. This doubling of the water content also reduced the rate of acetone hydrogenation by 2-fold vs that performed in the Burdick & Jackson acetone with its water content of <0.2%. The hydrogenation with the added water starts with an initial TOF of 0.29 ± 0.02 s^{-1}, and then slows as the reaction proceeds (Figure S-10 in the Supporting Information). After 11 h of hydrogenation, the solution is clear with black precipitates on the coating; that is, nanoclusters are formed, but are not stable and aggregate into big particles and, ultimately, into bulk metal.

A second control addressed the question of whether disiopropyl ether could be adsorbed by added molecular sieves, thereby obscuring its detection. This control was carried out simply by leaving a mixture of 0.95 equiv (95%) 2-propanol plus 0.025 equiv diisopropyl ether, produced in a standard conditions hydrogenation of normal acetone, over 0.2 g of molecular sieves. A ^{1}H NMR spectrum of the mixture after 8 h shows that the ratio of 2-propanol to diisopropyl ether does not change; that is, the diisopropyl ether is not selectively adsorbed by the added molecular sieves.

Acknowledgment. This work was supported by the Department of Energy, Office of Basic Energy Sciences, via DOE Grant FG06-089ER13998, and by a Fulbright Scholar Fellowship to S.Ö.

Supporting Information Available: Kinetic derivations, treatment of the composite reaction stoichiometry, experimental details, including calculations, figures, and tables. This material is available free of charge via the Internet at http://pubs.acs.org.

JA0437813

(51) Aplin, R. T.; Budzikiewicz, H.; Djerassi, C. *J. Am. Chem. Soc.* **1965**, *87*, 3180.